Detecting major growth stages of paddy rice using MODIS data

SUN Hua-sheng[1,2,3], HUANG Jing-feng[1,4], PENG Dai-liang[1,2]

1. *Institute of Agricultural Remote Sensing & Information Application, Zhejiang University, Zhejiang Hangzhou* 310029, *China*;
2.*Key Laboratory of Agricultural Remote Sensing and Information System, Zhejiang Province, Zhejiang Hangzhou*, 310029, *China*;
3. *College of Surveying and Mapping, Xuzhou Normal University, Jiangsu Xuzhou* 221116, *China*;
4. *Ministry of Education Key Laboratory of Environmental Remediation and Ecological Health, Zhejiang University, Zhejiang Hangzhou*, 310029, *China*

Abstract: Phenological information of paddy rice is important for area extraction and growth monitoring. The purpose of this study is to detect the major phenological stages of paddy rice over China using remote sensing data. Time-series Terra moderate-resolution imaging spectroradiometer (MODIS) Enhanced Vegetation Index (EVI) was smoothed with the low pass Fourier and wavelet filtering methods, then the stages of transplanting, beginning of tillering, heading, and maturation were obtained according to their characteristics. The paddy rice stages in 2005 derived from this study were significantly positive correlated and consistent with the statistical data ($P < 0.05$), and most of the absolute errors were less than 16 d. The methods presented in this study could be applied in other years, as well as the ability to generate the growth stages of other crops.

Key words: remote sensing, MODIS, EVI, paddy rice, growth stage, phenology

CLC number: TP701/S127 **Document code:** A

1 INTRODUCTION

Remote sensing technology has the advantages of acquiring images macroscopically and periodically. It is a feasible and efficient way to monitor phenological information at a large scale.

Previous researches have been implemented to acquire phenological information by remote sensing data. For example, Tucker *et al*. (1979) used hand-held radiometer data to monitor the development of corn and soybean in their test fields. As the development of high temporal resolution satellites, such as NOAA-AVHRR, EOS-MODIS and SPOT-VEGETATION and so on, remote sensing technology was widely used in the researches of vegetation phenology, e.g., Gallo and Flesch (1989) estimated the silking stage of corn by the AVHRR vegetation index data. Myneni and Tucker (1997) identified vegetation phenology to testify the global changes in the high-latitude regions of the northern hemisphere using the AVHRR data. Zhou *et al*. (2001) found that the average NDVI increased in Eurasia and north America by the AVHRR-NDVI and the recorded ground temperature data during 1981—1999. In addition, some studies indicated that the spring became earlier and the autumn turned later in the northern hemisphere (Defila & Clot, 2001; Menzel, 2000; Parmesan & Yohe, 2003; Roetzer *et al*., 2000; Root *et al*., 2003; Studer, 2005). Meanwhile, many methods were developed to determine the beginning and the end of growth. For example, the vegetation index threshold method was used by many researchers (Fischer, 1994; Justice *et al*., 1985; Lloyd, 1990; Markon *et al*., 1995). The moving average vegetation index method (Duchemin *et al*., 1999; Reed & Brown, 1994; Repo *et al*., 1996; Schwartz, 1999), i.e., it removes the noises by calculating the moving average of the time series, and then gets the intersection points of the smoothed line and the delayed one, which denote the beginning and the end of the growing season. The inflexion method (Moulin *et al*., 1997; Sakamoto *et al*., 2005; Zhang *et al*., 2003), i.e., if the derivative of the time-series curve is a positive number after zero, then the date can be regarded as the start of the growing season; while if it is a negative number before zero, then the date can be regarded as the end of the growth. The maximum slope method (Yu *et al*., 2003), i.e., it judges the growth stages by the magnitude of variation in the time series vegetation index. The method of seasonal midpoint of NDVI (Schwartz *et al*., 2002), i.e., it determines the beginning and the end of the growing season by judging the average of the maximum and the minimum in the smoothed time-series vegetation index. The method of plant phenology and satellite data combination (Chen *et al*., 2000, 2001), i.e., seasonal information is obtained by the integration of ground observation data and remote sensing data.

The detecting principle of the remote sensing method is based on the changes of the time-series vegetation index, because they represent the development of vegetation growth.

Received: 2008-07-31; **Accepted**: 2008-12-19

Foundation: Supported by the National Hi-Technology Research and Development Program (863) of China (No. 2006AA120101), and the National Natural Science Foundation of China (No. 40871158/D0106, and No. 40875070/D0509)

First author biography: SUN Hua-sheng (1980—), male, PhD, graduated from Zhejiang University, study on agricultural Remote Sensing and GIS Application, have published 5 papers. E-mail: sunhuasheng@126.com

Corresponding author: HUANG Jing-feng, E-mail: hjf@zju.edu.cn

This study attempted to detect the major growth stages of paddy rice in China using multi-temporal remote sensing data, and the results might provide useful references to the planting area detection and the growth monitoring of paddy rice at a large scale.

2 DATA AND METHODS

2.1 Study area

Paddy rice is one of the major staple food crops in China, which is planted in all provincial administrative units except Qinghai. According to the statistical data (NBSC, 2007), the sown area and the output of rice were stable in recent years. The average sown area was 30276 thousand hectares during 1990—2006, accounted for 27.8% of the average total grain area (108710 thousand hectares). The average output was 184353 tons, accounted for 39.3% of the average total grain output (468548 thousand tons). Therefore, rice plays an important role in meeting the national and the international grain requirement.

The cropping system of paddy rice is different in China because of the diversity of topography and climate, as well as the influence of economic factors. According to the agricultural statistics in recent years, double rice is dominant in Guangdong, Guangxi, Hainan, and Taiwan due to prolific rains and the high temperature; it is a mixed region of double and single rice in Fujian, Zhejiang, Jiangxi, Hunan, Hubei, and southern part of Anhui and Yunnan on account of less effective temperatures and the inferior quality of double rice; and single rice is dominant in the large regions beyond the above mentioned ones.

2.2 Data

The commonly used multi-temporal remote sensing data are NOAA-AVHRR, EOS-MODIS, SPOT-VEGETATION and so on. Considering the demands of spatial and temporal resolution, Terra MODIS data were chosen for rice growth stages detection in this study. The MODIS sensor has 36 spectral bands, 7 of which are designed for vegetation and land surface studies, the main parameters of the 7 bands are listed as Table 1. The MODIS Land Team provides a suite of standard MODIS products to the users from daily as well various composite products. All the data are available freely from the Land Processes Distributed Active Archive Center (LPDAAC) (http://lpdaac.usgs.gov).

Table 1 Main parameters of the first 7 bands of MODIS

Band	Range/nm	Name	Spatial resolution/m
1	620—670	red	250
2	841—876	NIR1	250
3	459—479	Blue	500
4	545—565	Green	500
5	1230—1250	NIR2	500
6	1628—1652	SWIR1	500
7	2105—2155	SWIR2	500

Because heavy clouds may affect the quality of the images, the 8-day composite images were used in this study to reduce the impact of clouds and to guarantee their high temporal resolution. MOD09A1 is the 8-day composite land surface reflectance product with 500 m spatial resolution. It includes the first 7 bands of MODIS, which are sensitive to land surface reflectance. Each pixel in the 8-day composite images is the best one in quality within 8 days on the basis of high observation coverage, low view angle, the absence of clouds, cloud shadows and aerosols (http://modis-land.gsfc.nasa.gov/surfrad.htm). The MODIS Land Data Operational Product Evaluation (LDOPE) facility (http://landweb.nascom.nasa.gov/cgi-bin/QA_WWW/newPage.cgi) provides a coordination mechanism for MODLAND's quality assessment (QA) activities (Roy *et al*., 2002). The band of QA at the pixel level is also provided together with the reflectance data in the products. Useful information is available on the basis of the description of the MODIS 8-day surface reflectance QA information (http://edcdaac.usgs.gov/modis/moyd09a1q1_qa_v4.asp) through binary calculation. Because it chooses the best pixels within 8 days in the MOD09A1 product, and the date selection could be regarded as a stochastic phenomenon from an overall perspective, so we used the middle date within the 8 days (official date, about the fourth day) to represent approximately the acquiring date of each composite image.

2.3 Methods

2.3.1 Selection of samples

To acquire rice phenological information over China, typical samples were selected in different regions with rice cultivation. In order to reduce the impact of the background as far as possible, we selected the bigger fields or some neighboring fields that can form into a big one in the image. In this study, 198 single rice samples and 87 double rice samples were selected. In addition, to validate the effect of the MODIS-derived results, we compared the results with the in situ observed data obtained from the agricultural meteorological observatories in the same year (131 effective single rice observatories and 87 effective double rice observatories were selected).

Because the positions of the agricultural meteorological observatories are different from the selected samples, in order to validate the effect of the MODIS-derived major rice growth stages, the distribution maps of rice growth stages in the whole country were obtained by spherical models of Ordinary Kriging interpolation in ArcGIS, and then the growth stages of the selected rice samples were obtained according to the maps as the ground truth data. Effective agricultural meteorological observatories were chosen as more as possible, because the accuracy of the interpolated results relies on the quantity and the spatial distribution of the samples. The errors of the interpolated results were controlled in the range less than 8 days in this study.

2.3.2 Pretreatment of the MODIS data

To amplify the difference between the features of interest and the background, index was used to enhance the vegetation

information. As the blue band is sensitive to the atmospheric conditions, it is used to adjust the reflectance in the red band as a function of the reflectance in EVI (Eq. (1)). EVI is an improved vegetation index, which accounts for the effects of residual atmospheric contamination and soil background, and it is much less sensitive to aerosols than the NDVI (Normalized Difference Vegetation Index), and not easy to reach the saturation in the regions covered with thick vegetation (Huete *et al*., 1997, 2002). For the LAI (leaf area index) of rice is high in the exuberant growth stage, so we chose EVI instead of NDVI for vegetation change detection.

$$\mathrm{EVI} = 2.5 \times \frac{\rho_{\mathrm{NIR1}} - \rho_{\mathrm{red}}}{\rho_{\mathrm{NIR1}} + 6.0 \times \rho_{\mathrm{red}} - 7.5 \times \rho_{\mathrm{blue}} + 1} = 2.5 \times \frac{B_2 - B_1}{B_2 + 6.0 \times B_1 - 7.5 \times B_3 + 1} \quad (1)$$

Although the MODIS 8-day composite surface reflectance products have been strictly pre-processed to reduce the impact of clouds, shadows and aerosols, obviously residual noises still exist in the regions with lasting heavy clouds, which have a big impact to the information extraction. There are some methods for noise removing, such as the simplest method of the moving median or average. Some other more complicated methods, such as the BISE algorithm (best index slope extraction) (Viovy *et al*., 1992), the Savitzky-Golay filter (Chen *et al*., 2004; Jönsson & Eklundh, 2004; Savitzky & Golay, 1964), the Fourier-based algorithm (Cihlar, 1996; Sellers *et al*., 1994), and the wavelet transform function (Gillian *et al*., 2008; Lu *et al*., 2007; Sakamoto *et al*., 2005). We attempted to get a very smooth curve after filtering to model the process of vegetation changes. In the above mentioned algorithms, the BISE method was designed for reducing noise in the NDVI time-series NOAA satellite data initially, and which can be used to process the MODIS data. The main purpose of the algorithm is to reconstruct the time-series vegetation index for reducing the impact of cloud contamination; however, the algorithm is not suitable for seasonal information acquirement. The Savitzky-Golay method essentially performs local polynomial regression in the time-series to determine the smoothed value for each point, the main advantage of this approach is that it tends to preserve features of the distribution such as peak values and width, which are usually flattened by the simple moving average model. However, lots of noises still exist in the filtered time-series profiles for seasonal information acquirement. The Fourier-based algorithm and the wavelet transform function can model the regular changes easily with smoothed curves by removing the high frequency (local variations) components and preserving the low frequency ones. Both of them can remove the noises as far as possible in the time-series, and model the regular seasonal changes so as to reflect the characteristics of seasonal variation, thus, the two algorithms are superior to other ones for rice phenological stages determination.

The method of DFT (discrete Fourier transform), sometimes called the finite Fourier transform (Cooley *et al*., 1969), is a Fourier transform widely employed in signal processing and related fields to analyze the frequencies contained in a sampled signal and to perform other operations such as convolutions. The DFT algorithm is slow, but it can be computed efficiently in practice using a FFT (fast Fourier transform) algorithm. For the Fourier transform function can be transformed into the composition of sines and cosines according to the Euler's formula, so the limitation of the Fourier transform is that it just fit for the periodic and stationary signals. While a wavelet is a kind of mathematical function used to divide a given function or continuous signal into different frequency components and study each component with a resolution that matches its scale. The advantages of using wavelet transform are that it has the abilities to represent functions that have discontinuities and sharp peaks, as well as accurately deconstruct or reconstruct finite, non-periodic or non-stationary signals. Because the seasonal change of rice is regular year by year, so both the Fourier transform and the wavelet transform algorithms are fit for removing the noises and modeling the changes.

In this study, we used the low pass filtering by FFT and DB (Daubechies) wavelet to cut off the noises in the time-series EVI. The phenological information of paddy rice was acquired by detecting the changes in the smoothed time-series EVI. Tests showed that the number of the window points in the low pass FFT filtering should be 4 for single rice, because the intervals of the peaks are large. If the number of the window points is too big (the larger of the window the smoother the curves will be), then the time-series curves will be flattened; if the number of the window points is too small, then there will be some peaks and cannot be used to determine the seasonal changes. Because the intervals of the peaks are small and the reflectance of late rice in the transplanting period tends to be impacted by the background, so the two peaks are not very clear. If the number of the window is too large, it might has only one peak in the profiles of the smoothed EVI and unable to get the seasonal information. Tests proved that the points of window should be 3 for double rice. We compared ten DB wavelets (N=1, N=2, …, N=10), and the results indicated that the DB10 wavelet (N=10) was better than the others. Similarly, considering the difference between single rice and double rice, the cutoff frequency was 85.0% to remove the high frequency components for single rice (the larger of the window the smoother the curves will be), while the cutoff frequency was 75.0% for double rice. Three typical samples for single rice and double rice were selected to display the effects of noise removing by FFT and wavelet transform filtering algorithms (Fig. 1).

2.3.3 Algorithms for detecting paddy rice phenological stages

The existent period of paddy rice is from transplanting time to harvest time. In order to transplant rice seedlings, and to guarantee the healthy growth, rice fields are filled with persistent water since the flooding period because of the special physiological property of the crop. Rice is easy to be separated from other crops according to the characteristic. Therefore, the transplanting period is significant for rice identification using remote sensing technology. The period from the beginning of

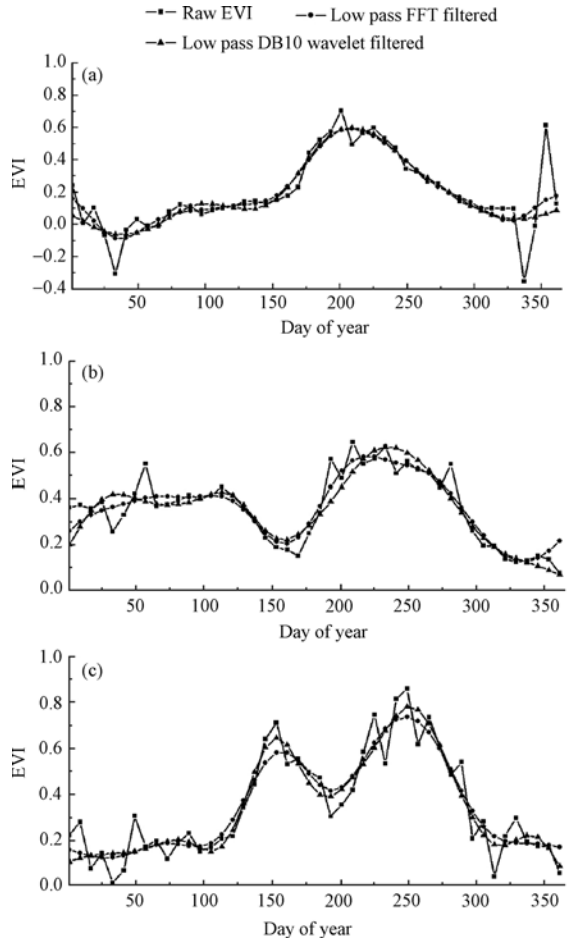

Fig. 1 Typical time-series EVI profiles of rice at selected sites in 2005, and the results of the low pass FFT and DB10 wavelet filtering
(a) Single rice in Heilongjiang (45°44′48″N, 132°40′06″E); (b) Other crop (winter wheat or oilseed rape) and single rice in Jiangsu (32°17′41″N, 120°48′59″E); (c) Double rice in Jiangxi (28°42′34″N, 116°11′36″E)

tillering to the maturation is significant to the crop growth monitoring using remote sensing technology, because it is crucial to the development and the ultimate yield of rice.

EVI reaches the minimum because of high soil moisture in the transplanting period, and the seedlings turn green and EVI has little increase in several days, so rice transplanting period can be detected by this characteristic. About one to two weeks after transplanting, rice turns into the tillering period. The tillering period is the beginning of the development of rice root and leaf systems, since then EVI increases rapidly. The vegetative development of rice reaches the maximum till the heading period, and then rice changes its growth phase from vegetative growth to reproductive growth. The nutrients are transferred into the seeds and EVI decrease gradually. In the maturation period, leaves lost most of the chlorophyll and begin to wither rapidly, and the vegetation index reaches the minimum in the harvest time. The characteristics of the major growth stages in smoothed time-series EVI are shown in Fig. 2. According to the above mentioned characteristics of each growth stage, the major rice growth stages can be detected through remote sensing technology.

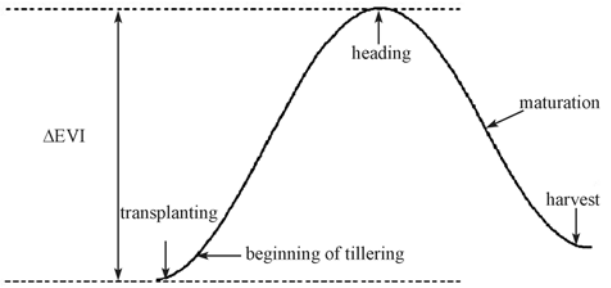

Fig. 2 Diagram showing the characteristics of major growth stages of paddy rice in smoothed time-series EVI

Paddy rice has different characteristics in different growth stages, and the previous methods were summarized and each growth stage was detected by separate method. According to the multi-temporal remote sensing data of the single and double rice samples, the detecting method of each stage was depicted as follows:

The inflexion method was used to identify rice heading period and transplanting period in this study. The maximum of EVI (EVI_{max}) and the minimum of EVI (EVI_{min}) were determined from the smoothed time-series EVI processed by the low pass Fourier and wavelet filtering (tests showed that the minimum was set to 0.15 forcibly when the value is lower than 0.15), and ΔEVI ($\Delta EVI = EVI_{max} - EVI_{min}$) was calculated. The date with the maximum is the heading period (there is only one maximum for single rice in a year, while there are two maximums for double rice). The transplanting period was identified after the heading period was determined. The date with the minimum can be regarded as the transplanting period when it appears before the heading period. If it appears after the heading period, then the date can be regarded as harvest period (the harvest time was not detected in the study).

The transplanting period is the date with the minimum if it is before the heading period, while if it is after the heading period, the date can be regarded as harvest (the harvest time was not detected in this study).

The relative vegetation index threshold method was used to determine the beginning of tillering. This method depends on the relative extent of EVI (percentage), so the impact of the background in different regions could be avoided. Tests indicated that if the total increment of EVI is over 10% of ΔEVI since the transplanting period, then the date could be regarded as the beginning of tillering.

As for rice maturation period, it could be identified by the maximum slope method. The maturation period could be identified by comparing the decrement of EVI between the present date and the previous date, the date with the biggest decrement could be regarded as the maturation period.

The process for the identification of the major growth stages of paddy rice using MODIS data is shown in Fig. 3 according to the above mentioned description.

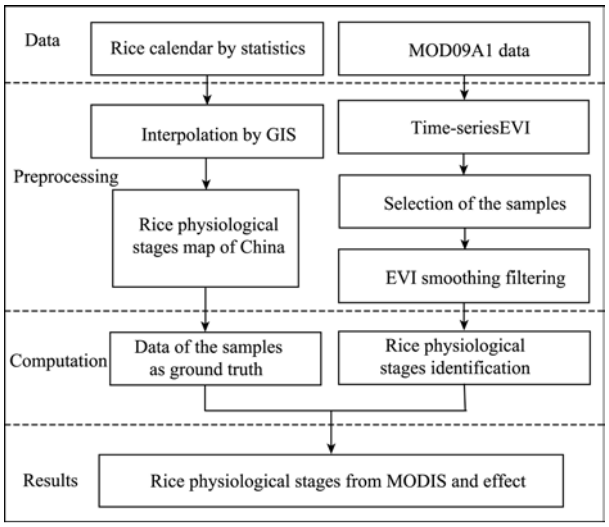

Fig. 3 Flowchart for the identification of the major growth stages of paddy rice using MODIS data

3 RESULTS

The stages of rice transplanting, beginning of tillering, heading, and maturation could be acquired by the above mentioned algorithms. The meteorological data were used to validate the MODIS derived results. In this study, we analyzed the results of 2005 as a case study to show the correlations. The comparisons between the MODIS-derived rice phenological stages and the meteorological data in 2005 are shown in Fig. 4, Fig. 5 and Fig. 6.

The results in Fig. 4, Fig. 5 and Fig. 6 showed that most of the absolute errors of the four major growth stages derived from the low pass FFT and wavelet filtered time-series EVI data were less than 16 d. F-tests were applied to make a further analysis of the consistency between them. Analyses indicated that all of the results had significant consistency at the level of 0.05, so the MODIS-derived results were reliable. In addition, the root mean square errors (RMSE) were calculated to show the differences by the low pass FFT and DB10 wavelet filtered EVI on the hypothesis that the meteorological statistics are the ground truth (Table 2).

According to the above analyses, the results derived from the low pass FFT and DB10 wavelet filtered EVI data were consistent approximately, though Sakamoto *et al*. reported that the wavelet transform performed better than the Fourier transform to detect the seasonal information of paddy rice in Japan. The study showed that heavy clouds had a big impact on the time-series EVI in some regions. Because wavelet filtering can model non-periodic or non-stationary signals, so the method is more sensitive to the local changes of the signals caused by noises and easy to have bigger errors. The changes of the rice growth has strong periodicity in a year, so the low pass Fourier transform algorithm is also useful to model the periodic signals, and sometimes the results derived from the algorithm might be better. In conclusion, the results derived from the two above filtering methods were close.

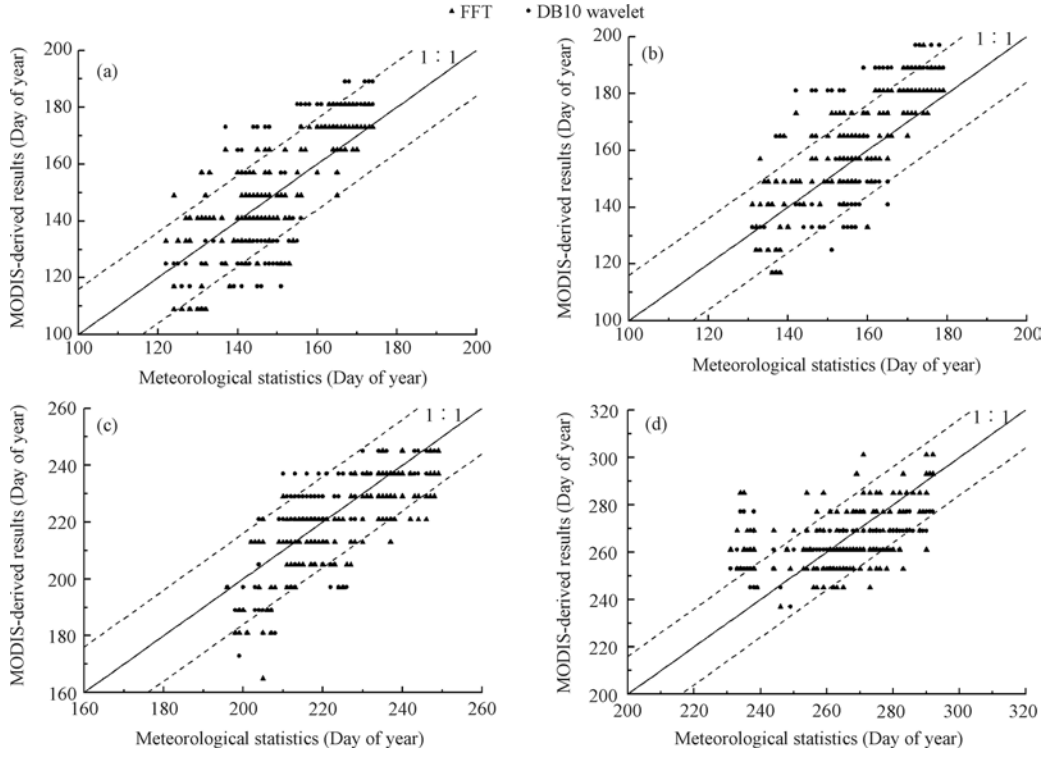

Fig. 4 Correlations between the MODIS-derived rice phenological stages and the meteorological data for single rice in 2005
(a) Transplanting; (b) Tillering; (c) Heading; (d) Maturation. (The dash lines in the above plots are the boundaries with errors of ±16 days.)

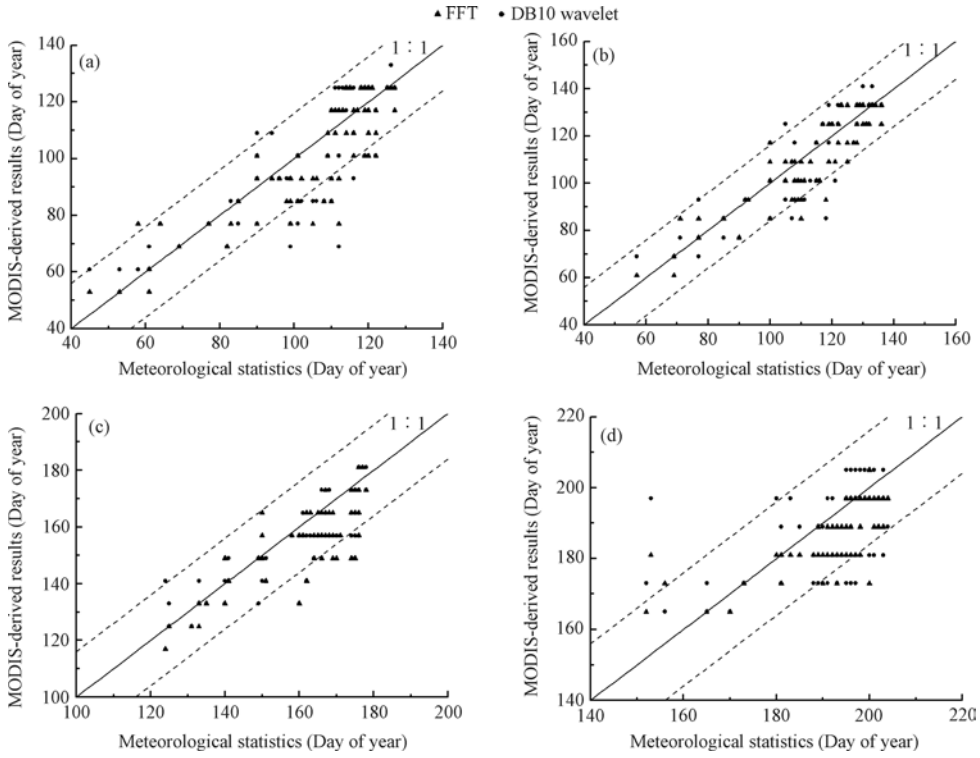

Fig. 5 Correlations between the MODIS-derived rice phenological stages and the meteorological statistics for early rice in 2005
(a) Transplanting; (b) Tillering; (c) Heading; (d) Maturation. (The dash lines in the above plots are the boundaries with errors of ±16 days.)

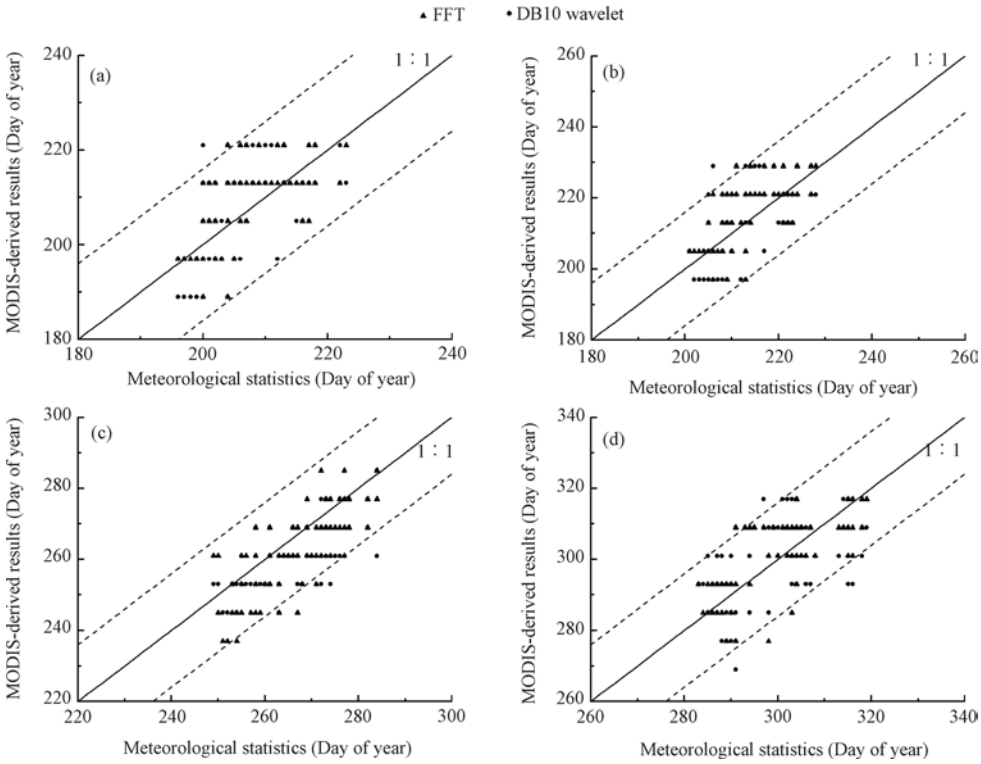

Fig. 6 Correlations between the MODIS-derived rice phenological stages and the meteorological statistics for late rice in 2005
(a) Transplanting; (b) Tillering; (c) Heading; (d) Maturation. (The dash lines in the above plots are the boundaries with errors of ±16 days.)

4 DISCUSSION AND CONCLUSIONS

The stages of transplanting, beginning of tillering, heading, and maturation were obtained using the time-series EVI data smoothed by the low pass Fourier and wavelet filtering. The above analyses indicated that both of the algorithms were useful to extract the growth stages information. The sources of the errors were discussed as follows: Firstly, the 8-day composite

Table 2 Comparison of the root mean square errors of the phenological date by the low pass FFT and DB10 wavelet filtered EVI on the hypothesis that the meteorological statistics are the ground truth data

Planting system	Growth stage	FFT/d	DB10 wavelet/d
Single rice	Transplanting	10.7	16.2
	Tillering	11.1	15.9
	Heading	11.2	11.5
	Maturation	14.6	12.4
Early rice	Transplanting	11.6	12.6
	Tillering	8.9	10.5
	Heading	9.5	10.1
	Maturation	9.6	12.9
Late rice	Transplanting	7.2	9.3
	Tillering	7.8	9.5
	Heading	9.3	8.8
	Maturation	7.9	10.4

images were used instead of the daily ones to reduce the impact of clouds and the middle date within the 8d (about the fourth day) were used to represent the acquiring date of each composite image, so this might cause an error of ±4d. Secondly, the locations of the selected rice samples were different from the locations of the agricultural meteorological stations, and the interpolated results might be different from the real values. Thirdly, statistical sampling method was used to collect the growth stages information, and the results might be different even in a small region because of individual fields.

Cloud detection showed that lots of cloud contaminated pixels still existed in the 8-day composite images. If the 16-day (a revisit period of Terra) composite images were used, the impact of clouds might be decreased. However, the temporal resolution might be decreased at the same time, and the error of the real date and the official date increased to ±8d. While the growth period is short for crops, and usually they can only exist in several months in the fields, so the precision of the results derived from the 16-day composite images might be too low. If the daily images were used in the regions with little cloud contamination, then the precision of the results might be better for the improvement of the temporal resolution.

The above analyses indicated that the 8-day composite MODIS data were useful to the growth stages detection of paddy rice. Clouds or other factors might disturb the time-series EVI data, although most of the noises can be removed by the low pass FFT and wavelet filtering, they still have big impacts on the smoothed results. According to the comparisons between the MODIS-derived results and the meteorological statistics, most of the absolute errors of the results were less than 16d, so the results were reliable. The detecting methods in this study could be used to extract rice growth stages in other years, and the results might provide useful references to the planting area detection and the growth monitoring of paddy rice. In addition, the methods in this study might be able to extract the growth stages of other crops according to their characteristics potentially.

Acknowledgement: The in situ field survey data of rice growth calendar are provided by National Meteorological Bureau of China; the MODIS data used in this study are distributed freely by the Land Processes Distributed Active Archive Center (LP DAAC), located at the U.S. Geological Survey (USGS) Center for Earth Resources Observation and Science (EROS) (http://lpdaac.usgs.gov). The authors are very grateful to their generous supports.

REFERENCES

Chen J, Jonsson P, Tamura M, Gu Z, Matsushita B and Eklundh L. 2004. A simple method for reconstructing a high-quality NDVI time-series data set based on the Savitzky-Golay filter. *Remote Sensing of Environment*, **91**: 332—344

Chen X, Tan Z J, Schwartz M D and Xu C. 2000. Determining the growing season of land vegetation on the basis of plant phenology and satellite data in Northern China. *International Journal of Biometeorology*, **44**: 97—101

Chen X, Xu C and Tan Z. 2001. An analysis of relationships among plant community phenology and seasonal metrics of Normalized Difference Vegetation Index in the northern part of the monsoon region of China. *International Journal of Biometeorology*, **45**(4): 170—177

Cihlar J. 1996. Identification of contaminated pixels in AVHRR composite images for studies of land biosphere. *Remote Sensing of Environment*, **56**: 149—153

Cooley J, Lewis P and Welch P. 1969. The finite Fourier transform . *IEEE Trans. Audio Electroacoustics*, **17**(2): 77—85

Defila C and Clot B. 2001. Phytophenological trends in Switzerland. *International Journal of Biometeorology*, **45**: 203—207

Duchemin B, Goubicr J and Courrier G. 1999. Monitoring phenological key stages and cycle duration of temperate deciduous forest ecosystems with NOAA/AVHRR data. *Remote Sensing of Environment*, **67**: 68—82

Fischer A. 1994. A model for the seasonal variations of vegetation indices in coarse resolution data and its inversion to extract crop parameters. *Remote Sensing of Environment*, **48**(2): 220—230

Gallo K P and Flesch T K. 1989. Large-area crop monitoring with the NOAA AVHRR: Estimating the silking stage of corn development. *Remote Sensing of Environment*, **27**: 73—80

Gillian L G, John F M, Jerry M , Aline G, Carlos C C and Carlos E P C. 2008. Wavelet analysis of MODIS time series to detect expansion and intensification of row-crop agriculture in Brazil. *Remote Sensing of Environment*, **112**: 576—587

Huete A R, Didan K, Miura T, Rodriguez E P R, Gao X and Ferreira L G. 2002. Overview of the radiometric and biophysical performance of the MODIS vegetation indices. *Remote Sensing of Environment*, **83**: 195—213

Huete A R, Liu H Q, Batchily K and van Leeuwen W. 1997. A comparison of vegetation indices global set of TM images for

EOS-MODIS. *Remote Sensing of Environment*, **59**: 440—451

Jönsson P and Eklundh L. 2004. TIMESAT — a program for analyzing time-series of satellite sensor data. *Computers & Geosciences*, **30**: 833—845

Justice C O, Townshend J R G, Holben B N and Tucker C J. 1985. Analysis of the phenology of global vegetation using meteorological satellite data. *International Journal of Remote Sensing*, **6**(8): 1271—1318

Lloyd D. 1990. A phenological classification of terrestrial vegetation cover using shortwave vegetation index imagery. *International Journal of Remote Sensing*, **11**: 2269—2279

Lu X, Liu R, Liu J and Liang S. 2007. Removal of noise by Wavelet method to generate the high-quality time series of terrestrial MODIS products. *Photogrammetric Engineering and Remote Sensing*, **73**(10): 1129—1139

Markon C J, Fleming M D and Binnian E F. 1995. Characteristics of vegetation phenology over the Alaskan landscape using AVHRR time-series data. *Polar Record*, **31**: 179—190

Menzel A. 2000. Trends in phenological phases in Europe between 1951 and 1996. *International Journal of Biometeorology*, **44**: 76—81

Moulin S, Kergoat L, Viovy N and Dedieu G. 1997. Global-scale assessment of vegetation phenology using NOAA/AVHRR satellite measurements. *Journal of Climate*, **10**: 1154—1170

Myneni R B and Tucker C J. 1997. Increased plant growth in the northern high latitudes from 1981 to 1991. *Nature*, **386**: 698—702

NBSC (National Bureau of Statistics of China). 2007. Statistical Yearbook of China. China Statistics Press

Parmesan C and Yohe G. 2003. A globally coherent fingerprint of climate change impacts across natural systems. *Nature*, **421**: 37—42

Reed B C and Brown J F. 1994. Measuring phenological variability from satellite imagery. *Journal of Vegetation Science*, **5**: 703—714

Repo T, Hänninen H and Kellomäki S. 1996. The effects of long-term elevation of air temperature and CO_2 on the frost hardiness of Scots pine. *Plant Cell and Environment*, **19**: 209—216

Roetzer T, Wittenzeller M, Haeckel H and Nekovar J. 2000. Phenology in central Europe-differences and trends of spring phenophases in urban and rural areas. *International Journal of Biometeorology*, **44**: 60—66

Root T L, Price J T, Hall K R, Schneider S H, Rosenzweig C and Pounds J A. 2003. Fingerprints of global warming on wild animals and plants. *Nature*, **421**: 57—60

Roy D P, Borak J S, Devadiga S, Wolfs R E, Zheng M and Descloitres J. 2002. The MODIS land product quality assessment approach. *Remote Sensing of Environment*, **83**: 62—76

Sakamoto T, Yokozawa M, Toritani H, Shibayama M, Ishitsuka N and Ohno H. 2005. A crop phenology detection method using time-series MODIS data. *Remote Sensing of Environment*, **96**: 366—374

Savitzky A and Golay M J E. 1964. Smoothing and differentiation of data by simplified least squares procedures. *Analytical Chemistry*, **36**(8): 1627—1639

Schwartz M D, Reed B C and White M A. 2002. Assessing satellite-derived start-of-season measures in the conterminous USA. *International Journal of Climatology*, **22**(14): 1793—1805

Schwartz M D. 1999. Advancing to full bloom: planning phenological research for the 21st century. *International Journal of Biometeorology*, **42**(3): 113—118

Sellers P J, Tucker C J, Collatz G J, Los S O, Justice C O, Dazlich D A and Randall D A. 1994. A global 1° by 1° NDVI data set for climate studies: Part II. The generation of global fields of terrestrial biophysical parameters from the NDVI. *International Journal of Remote Sensing*, **15**(17): 3519—3545

Studer S, Appenzeller C and Defila C. 2005. Inter-annual variability and decadal trends in Alpine spring phenology: a multivariate analysis approach. *Climate Change*, **73**: 395—414

Tucker C J, Elgin J H Jr, McMurtrey J E and Fan C J. 1979. Monitoring corn and soybean crop development by remote sensing techniques. *Remote Sensing of Environment*, **8**(3): 237—248

Viovy N, Arino O and Belward A. 1992. The Best Index Slope Extraction (BISE): A method for reducing noise in NDVI time-series. *International Journal of Remote Sensing*, **13**(8): 1585—1590

Yu F, Price K P, Ellis J and Shi P. 2003. Response of seasonal vegetation development to climatic variations in eastern central Asia. *Remote Sensing of Environment*, **87**(1): 42—54

Zhang X, Friedl M A, Schaaf C B, Strahler A H, Hodges J C F, Gao F, Reed B C and Huete A. 2003. Monitoring vegetation phenology using MODIS. *Remote Sensing of Environment*, **84**: 471—475

Zhou L, Tucker C J, Kaufmann R K, Slayback D, Shabanov N V and Myneni R B. 2001. Variations in northern vegetation activity inferred from satellite data of vegetation index during 1981 to 1999. *Journal of Geophysical Research*, **106**: 20069—20083

利用 MODIS 数据识别水稻关键生长发育期

孙华生[1,2,3], 黄敬峰[1,4], 彭代亮[1,2]

1. 浙江大学 农业遥感与信息技术应用研究所, 浙江 杭州 310029;
2. 浙江省农业遥感与信息技术应用重点研究实验室, 浙江 杭州 310029;
3. 徐州师范大学测绘学院 江苏 徐州 221116;
4. 环境修复与生态健康教育部重点实验室, 浙江 杭州 310029

摘 要: 利用遥感方法提取中国范围内的水稻关键生长发育期。首先, 对时间序列 Terra MODIS-EVI(Enhanced Vegetation Index)进行傅里叶和小波低通滤波平滑处理, 然后, 根据水稻在移栽期、分蘖初期、抽穗期和成熟期的 EVI 变化特征, 实现对各个生长发育期的识别。通过将利用 2005 年 MODIS 数据识别的结果与当年气象台站的地面观测资料进行比较, 采用本研究中的识别方法得出的水稻各个生长发育期的绝对误差大部分小于 16d, 经过 F 检验表明提取的结果与地面观测资料在 0.05 水平下具有显著一致性。研究中的信息提取方法可被用于其他年份的水稻生长发育期识别, 根据其他作物的生长发育特点, 也可能适合于提取其他作物的生长发育期。

关键词: 遥感, MODIS, EVI, 水稻, 生长发育期, 物候

中图分类号: TP701/S127 文献标识码: A

1 引 言

遥感技术获取植被的季相变化信息已经成为一种重要的替代手段。遥感技术具有宏观性和周期性的特点, 在大尺度的植被物候期观测方面发挥了非常重要的作用。

利用遥感方法对植被物候期进行识别方面, 很多学者进行了大量的研究。例如, Tucker 等(1979)在地面田间试验中利用手持辐射仪数据监测玉米、大豆的生育期。随着高时间分辨率的卫星传感器的发展, 如 NOAA-AVHRR(以下简称 AVHRR)、EOS-MODIS(以下简称 MODIS)和 SPOT-VEGETATION(以下简称 VEGETATION)等, 此类卫星遥感数据已广泛应用于植被物候期识别研究。例如, Gallo 和 Flesch(1989)利用 AVHRR 植被指数数据估测玉米吐丝期, Myneni 和 Tucker(1997)利用 AVHRR 数据对北半球高纬度地区进行植被物候期的识别以反映全球环境变化。Zhou 等(2001)利用 1981—1999 年期间的 AVHRR 数据计算的 NDVI 和地面记录的地表温度数据发现欧亚大陆和北美大陆的平均 NDVI 增加。还有, 很多研究通过时间序列的物候信息表明, 在全球气候变化的影响下, 北半球的春季来得更早, 秋季变得更晚(Defila & Clot, 2001; Menzel, 2000; Parmesan & Yohe, 2003; Roetzer 等, 2000; Root 等, 2003; Studer, 2005)。同时, 也发展了许多判断植物生长季开始和结束的方法。例如, 植被指数阈值法, 即通过设定植被指数的临界值确定生长季节的开始和结束的方法, 许多学者采用该方法确定生长季节的开始和结束日期(Fischer, 1994; Justice 等, 1985; Lloyd, 1990; Markon 等, 1995); 植被指数滑动移动平均法(Duchemin 等, 1999; Reed & Brown, 1994; Repo 等, 1996; Schwartz, 1999), 它首先通过滑动移动平均法进行平滑处理以去除噪声, 然后利用延迟的平滑曲线与其平滑曲线本身的交点来表示生长季节的开始和结束日期的方法; 转折点法(Moulin 等, 1997; Sakamoto 等, 2005; Zhang 等, 2003); 最大变化斜率法(Yu 等, 2003), 即将时间曲线导数从 0 到正数的转折点定义为生长季节的开始期, 将从负值到 0 的转折点定义为生长季节的结束期的方法, 即根据植被在时间序列的变化幅度来判断生长季的方法; 季节 NDVI 中点法(Schwartz 等, 2002), 即利用平滑的判断时间序列 NDVI 最大值和最小值的均值来判

收稿日期: 2008-07-31; 修订日期: 2008-12-19

基金项目: 国家“863”课题(编号: 2006AA120101)和国家自然科学基金项目(编号: 40871158/D0106, 40875070/D0509)。

第一作者简介: 孙华生(1980—), 男, 浙江大学博士, 从事农业遥感和信息技术应用研究, 已发表论文 5 篇。E-mail: sunhuasheng@126.com。

通讯作者: 黄敬峰, E-mail: hjf@zju.edu.cn。

断生长季的开始和结束的方法; 植被物候期的频率分布与遥感数据相结合法(Chen 等, 2000, 2001), 即根据地面观测和遥感方法相结合的方法判断植被物候期的方法。

2 研究数据与方法

2.1 研究区概况

水稻是中国最重要的粮食作物之一, 水稻种植遍布全国, 除了青海省以外, 其他各省(市、自治区)均有水稻种植。据 2007 年中国统计数据(NBSC, 2007), 中国的水稻种植面积和产量一直比较稳定, 1990—2006 年全国水稻平均播种面积为 3027.6 万 hm^2, 只占粮食平均播种面积 10871.0 万 hm^2 的 27.8%, 而平均总产量却为 18435.3 万 t, 占粮食总产量 46854.8 万 t 的 39.3%。因此, 水稻种植对满足国内乃至世界的粮食需求至关重要。由于地形和气候条件的差异, 以及受到经济效益的影响, 中国水稻的种植制度有很大差异。根据近年来的农业统计资料, 在广东、广西、海南和台湾地区, 由于全年高温湿润, 主要种植双季稻; 在云南南部、福建、浙江、江西、湖南、湖北和安徽南部地区, 由于积温较以上的区域少, 而且由于双季稻的质量较差, 所以该地区既有双季稻又有单季稻, 是单季与双季的过渡地区; 在以上区域以外的其他地区, 绝大部分以单季稻为主。

2.2 研究采用的数据

常用多时相遥感数据主要有 AVHRR、MODIS 和 VEGETATION 等, 考虑到数据的空间分辨率和时间分辨率的要求, 研究选用 Terra MODIS 数据作为识别水稻生长发育期的资料。MODIS 数据的 36 个波段中前 7 个波段主要用于陆地和植被的研究(表 1)。MODIS 陆地工作组(MODIS Land Team)提供一系列的 MODIS 产品, 所有数据可以通过 LPDAAC (Land Processes Distributed Active Archive Center)免费获取(http://lpdaac.usgs.gov)。

由于云覆盖对图像的质量产生重要影响, 为了最大限度地降低云的影响, 保证图像较高的时间分辨率, 研究采用了 8d 合成的 MODIS 数据。MOD09A1 的陆地表面反射率产品, 该产品包括了对陆地表面地物反射比较敏感的前 7 个波段, 空间分辨率为 500 m, 数据产品采用了 8d 合成法以降低云及其阴影、气溶胶等因素的影响, 该产品图像的每个像元从 8d 中选择观测角最小、无云及其阴影、无气溶胶干扰的像元, 并且产品经过几何精校正、辐射校正和去除薄云处理(http://modis-land.gsfc.nasa.gov/surfrad.htm), 同时由 MODIS 产品质量评价工作组 (LDOPE, http://landweb.nascom.nasa.gov/cgi-bin/QA_WWW/newPage.cgi)提供了每个像元的质量评价信息(QA)(Roy 等, 2002), 质量评价信息与各个波段的反射率数据一起提供给用户。MOD09A1 的 QA 信息可通过其描述(http://edcdaac.usgs.gov/modis/moyd09a1q1_qa_v4.asp)转换为有效的信息。由于 MOD09A1 为 8d 合成的产品, 数据选择标准是在 8d 中质量最好的, 所以在不同区域选择的日期是不确定的, 但从整体角度看, 日期的选择可以被看作是一种随机现象, 因此, 可利用这 8d 中的中间值(约第 4 天)近似地代表图像的实际获取日期。

表 1 **MODIS** 传感器前 7 个波段的主要参数

波段	范围/nm	名称	空间分辨率/m
1	620—670	红光波段	250
2	841—876	近红外 1 波段	250
3	459—479	蓝光波段	500
4	545—565	绿光波段	500
5	1230—1250	近红外 2 波段	500
6	1628—1652	短波红外 1 波段	500
7	2105—2155	短波红外 2 波段	500

2.3 研究方法

2.3.1 样点的选择

为了能够获取全国范围的水稻季相信息, 在全国不同区域有水稻分布的区域内抽取典型的试验样区。由于 MODIS 数据的分辨率较低, 为了尽可能降低背景的影响, 选取田块较大或者有较多田块连续可以构成较大的田块作为样点。最终在全国范围内确定了 198 个单季稻样点, 87 个双季稻样点。为了对利用遥感数据获取的结果进行验证, 与国家气象局设定的气象台站(选取 131 个有效的单季稻台站和 79 个有效的双季稻台站)同年的实际观测资料进行对比分析。由于气象台站的空间位置与所选取的典型试验样点的空间位置并不一致, 为了验证利用 MODIS 数据进行水稻关键发育期识别的效果, 根据气象台站对各个生长发育期的观测数据, 利用 ArcGIS 的空间插值功能, 采用 Ordinary Kriging 插值法进行插值处理, 选取球状模型拟合变异函数, 从而得到全国范围内的水稻生长发育期分布图, 根据此结果确定试验样点的水稻发育期。由于插值结

果的精度取决于气象台站的数量和空间分布，因此研究尽可能多地保留有效的气象台站数据。研究选取的气象台站的数量和空间分布可保证插值结果的误差均在 8d 以内。

2.3.2 数据预处理

为了扩大感兴趣地物与其背景的差异，研究采用了指数法对植被进行增强处理。由于蓝波段对大气条件比较敏感，所以它在 EVI 中被用来调整红波段的反射值。EVI 是增强的植被指数，因为它消除了残留的大气干扰和土壤背景的影响，与 NDVI 相比，EVI 对气溶胶和土壤背景的影响更不敏感，而且在植被茂密的地区更不容易饱和(Huete 等，1997, 2002)。由于水稻在生长最旺盛的时期的叶面积指数(LAI)相当高，所以 EVI 更适合对水稻的生物量变化进行监测，研究选取 EVI 作为识别水稻植被变化的依据，其计算方法见公式(1)。

$$\begin{aligned}\mathrm{EVI} &= 2.5 \times \frac{\rho_{\mathrm{NIR1}} - \rho_{\mathrm{red}}}{\rho_{\mathrm{NIR1}} + 6.0 \times \rho_{\mathrm{red}} - 7.5 \times \rho_{\mathrm{blue}} + 1} \\ &= 2.5 \times \frac{B_2 - B_1}{B_2 + 6.0 \times B_1 - 7.5 \times B_3 + 1} \end{aligned} \quad (1)$$

尽管 MODIS 8d 合成的地表反射率产品经过了严格的去云、云阴影和气溶胶的处理，然而，在多云的地区仍然存在大量的残留噪声，这些噪声对信息获取有很大的影响。为了进一步降低云的影响，有很多方法可以处理时间序列中的噪声，比如简单的滑动平均或者滑动均值法，还有更复杂的 BISE (best index slope extraction)算法(Viovy 等，1992), Savitzky-Golay 滤波算法(Chen 等，2004; Jönsson & Eklundh, 2004; Savitzky & Golay, 1964), 傅里叶平滑算法(Cihlar, 1996; Sellers 等，1994), 小波平滑算法(Gillian 等, 2008; Lu 等, 2007; Sakamoto 等, 2005)等。研究希望在获取作物季相变化信息时，通过滤波去噪后得到一条非常平滑的曲线，用来模拟植被的变化过程。在以上的算法中，BISE 是针对 NOAA 卫星获取数据计算的 NDVI 的去噪算法，它也可以用来处理 MODIS 数据，主要是对时间序列植被指数图像进行重构，以降低对云覆盖等原因造成的图像质量下降，然而这种算法对获取作物的季相信息并不适合；Savitzky-Golay 滤波法是通过局部多项式回归建立模型来判断时间序列的各个点的数据，该算法与简单的滑动平均相比，它可以更好地去除局部变化大的噪声点并保留原始数据的峰值和宽度，而对简单的滑动平均处理中通常会把这些信息给去除了，然而这对获取作物季相信息仍然存在大量的噪声；而傅里叶和小波低通滤波算法可以更好地去除高频(局部变化大的)分量(噪声)，保留低频的分量，最大限度地去除时间序列中的噪声，很容易地模拟出水稻的这种有规律的季节变化，反映出其季相变化特征。因此，在获取水稻季相变化信息时，傅里叶算法和小波算法比其他算法更优越。

离散傅里叶变换有时也叫做有限傅里叶变换(Cooley 等, 1969)，它在信号处理和相关的领域中被广泛地应用于分析样本信号的频率和进行卷积运算，由于离散傅里叶变换运行速度较慢，它一般通过快速傅里叶算法(FFT)进行计算。傅里叶函数可以转换为正弦和余弦函数的组合，因此，也就很容易理解它的限制性，即它仅适用于周期的和平稳的信号；而小波函数可以把连续信号分解为不同频率分量的函数，每个分量与一个尺度相对应。小波变换与傅里叶变换相比较，小波可以更好地表示不连续的和局部变化的信号，它可以用于非周期的和不平稳信号的重构。由于水稻在不同年份的季相变化是一种规律性较强的、相对比较稳定的变化，所以傅里叶和小波均能够模拟这种变化趋势。

研究采用 FFT 低通滤波法和 Daubechies 小波低通滤波去除时间序列 EVI 中的噪声。因此，水稻的季相信息就可以通过检测时间序列的 EVI 变化得到。试验表明：利用 FFT 低通滤波法去噪处理时，对单季稻而言，由于作物的发育期间隔较大，滤波窗口设定为 4 时滤波的效果最好。如果滤波窗口过大(窗口越大曲线越平滑)，时间序列中的波谷和波峰就被削平，如果滤波窗口过小则会出现几个波峰，就识别不出季相变换的规律；而对双季稻而言，因为两个波峰相隔较短，而且在晚稻移栽期时稻田的反射光谱受背景的影响较大，所以两个波峰之间的区分不是非常明显，如果采用的滤波窗口过大，那么滤波后 EVI 剖面中就很有可能变为一个波峰，就反映不出季相变化的规律，试验表明窗口为 3 时比较适合。对小波低通滤波法，通过比较 10 种 Daubechies 小波(N=1, N=2, …, N=10)，结果表明 N=10 时的小波去噪效果最好。同样考虑单季稻和双季稻的季相变化差异，对单季稻设定的截止频率(cutoff frequency)为 85.0%(截止频率百分比越大曲线越平滑)，去除高频分量(噪声)，而对双季稻设定的截止频率为 75.0%，去除高频分量。图 1 为在单季稻区和双季稻区选取的 3 个具有代表性的样点，以说明 FFT 低通滤波和 Daubechies(N=10)小波(以下简称 DB10 小波)低通滤波的去噪效果。

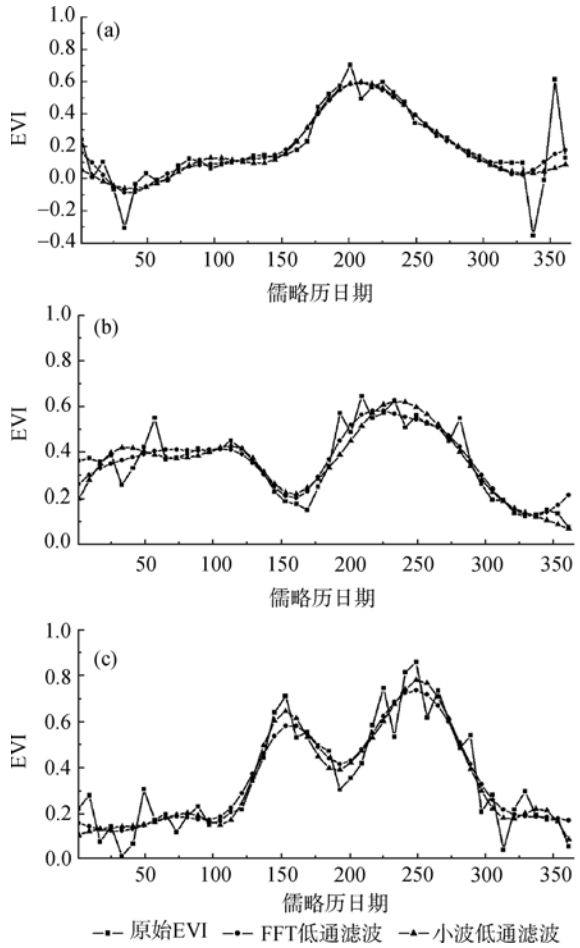

图 1 典型试验样点 2005 年的时间序列 EVI 剖面, 及 FFT 低通滤波与 DB10 小波低通滤波的效果

(a) 黑龙江省单季稻(45°44′48″N, 132°40′06″E); (b) 江苏省其他作物(冬小麦或油菜)和单季稻(32°17′41″N, 120°48′59″E); (c) 江西省双季稻(28°42′34″N, 116°11'36″E)

2.3.3 水稻关键生长发育期遥感识别的算法

在大田中, 水稻存在的时期是从插秧期一直到收获期。根据水稻的生理特性, 水稻在移栽以前稻田需要进行灌水以便于插秧和保证水稻正常生长, 利用这个特点可以很容易地与其他作物区分开来, 所以移栽期是判断水稻种植面积的最重要的时期; 而对利用遥感技术监测水稻生长发育最重要的时期是从分蘖初期(水稻根系和叶系发育的开始)到成熟期(发育基本停止)之间的这段时期, 因为这一段时间对水稻的长势状况和产量形成起着决定性的作用。

在水稻的移栽期, 由于存在大量水的原因 EVI 处于最小值, 在水稻移栽以后由于稻田出现秧苗, 并在几天内快速返青, 所以 EVI 略有增加, 因此可以根据这一特点确定移栽期; 在水稻移栽后的 1 到 2 周左右, 水稻进入分蘖期, 此时是水稻根系和叶系生长的开始, 从这时起 EVI 快速增加; 一直到抽穗期时水稻的营养生长已经达到了顶峰并开始转入生殖生长为主的阶段, 此时 EVI 达到最大值; 在抽穗期以后的阶段水稻植株内的养分逐渐转入到籽粒中, EVI 逐渐下降。在成熟期时叶片失去叶绿素而枯黄, 因此, 这个时期是植被指数下降速度最大的时期, 到收获期后植被指数几乎降到最低。对这几个发育时期在时间序列 EVI 中的变化特征可以通过图 2 来说明。因此, 可以根据以上描述的水稻各个生长阶段的特性, 通过遥感方法监测时间序列的植被指数变化实现对水稻的生长发育期的识别。

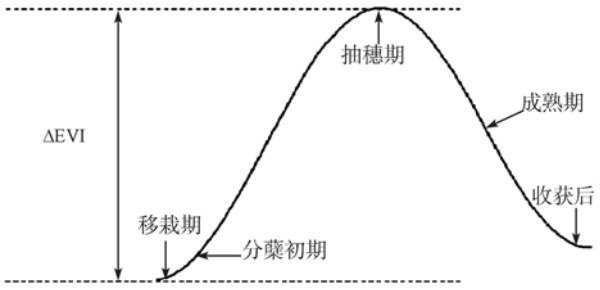

图 2 水稻主要生长发育期在平滑处理时间序列 EVI 中的特征示意图

由于水稻在不同的生育期表现出不同的特征。通过对前人研究成果的总结, 利用选取的单季稻和双季稻试验样点的多时相遥感数据, 对不同的发育期采用不同的识别方法, 实现全国范围内水稻生长发育期的识别。对它们分别采用的具体方法描述如下:

对水稻的抽穗期和移栽期, 研究采用转折点法进行识别。首先, 从利用傅里叶和小波低通滤波平滑后的时间序列 EVI 曲线中找出最大值 EVI_{max} 和最小值 EVI_{min}(试验表明, 当 EVI 小于 0.15 就将 0.15 强行设定为最小值), 再计算出最大值与最小值的差值 ΔEVI。其中, EVI_{max} 对应的时期即为抽穗期(对单季稻在一年中只有 1 个最大值, 而双季稻则有 2 个最大值); 在判断出抽穗期以后, 再判断出移栽期, 即如果 EVI_{min} 在抽穗期以前, 那么其对应的时期即为移栽期, 而如果 EVI_{min} 在抽穗期以后则为收获后的时期(因研究不考虑收获后的日期故将其舍弃)。

对分蘖初期, 研究采用植被指数的相对变化阈值法进行判断, 即通过判断 EVI 变化的相对幅度(即变化的百分数)来判断, 这样就可以避免在不同区域由于背景差异而导致的变化不一致问题。试验表明, 在 EVI 达到最大值前的某一时期, 当 EVI 从移栽期

开始增加到超过 ΔEVI 的 10%时，那么该时期可被认为是分蘖初期。

对成熟期，研究采用最大变化斜率法进行识别。在 EVI 达到最大值后，比较每一时期与前一时期的 EVI 的减少量，减少量最大的时期可被认为是成熟期。

综上所述，利用 MODIS 数据进行水稻关键生长发育期识别的整个流程如图 3。

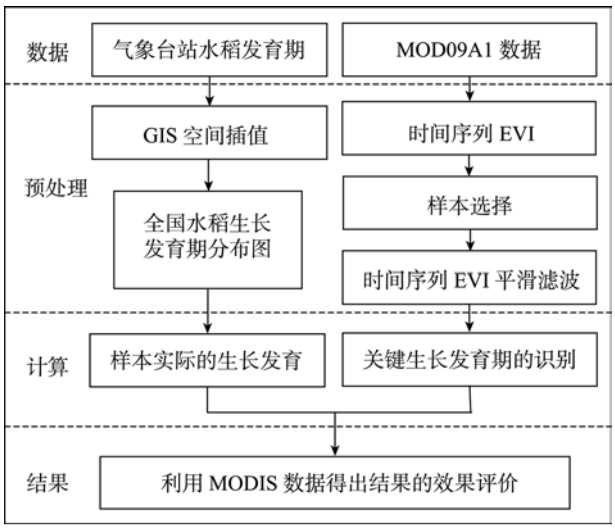

图3 利用MODIS数据识别水稻关键生长发育期的流程图

3 研究结果

根据以上描述的对不同时期采用算法，即可实现对水稻的移栽期、分蘖初期、抽穗期和成熟期识别。为了验证利用多时相 MODIS 数据对水稻关键生长发育期的识别效果，将识别结果与气象台站的观测数据进行比较。研究以 2005 年的比较结果为例，分析它们之间的相关性。利用 MODIS 数据的提取结果与气象台站的观测结果的比较见图 4、图 5 和图 6。

通过图 4、图 5 和图 6 的比较结果可以看出，利用 FFT 和小波低通滤波去噪处理的时间序列 EVI 数据对水稻的这 4 个关键生长发育期的识别结果绝大部分误差在±16d 之内。为了进一步比较它们的相关性，对二者进行 F 检验进一步分析其识别效果。通过对利用 MODIS 图像的识别结果与气象台站的观测结果进行相关性检验，以上结果均在 0.05 水平上表现出显著性，说明利用 MODIS 数据识别的结果是可靠的。此外，为了进一步比较利用 FFT 和小波低通滤波处理后的时间序列 EVI 对水稻各个生长发育期识别结果的准确性，将气象台站的观测数据作为真值，采用均方根误差(RMSE)反映出利用这两种方法提取结果的差异。其计算结果见表 2。

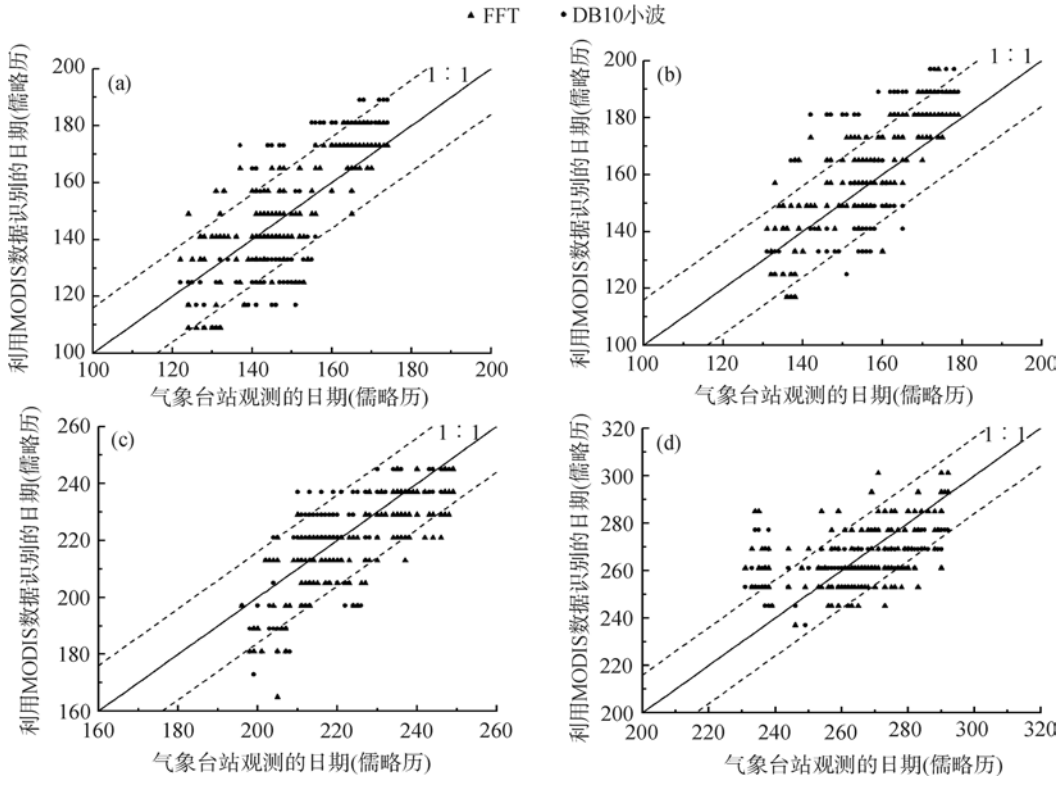

图 4 利用 MODIS 数据识别的 2005 年单季稻各个生长发育期与气象台站观测的各个生长发育期的比较结果

(a)移栽期; (b)分蘖初期; (c)抽穗期; (d)成熟期(图中的虚线是误差为±16d 的边界线)

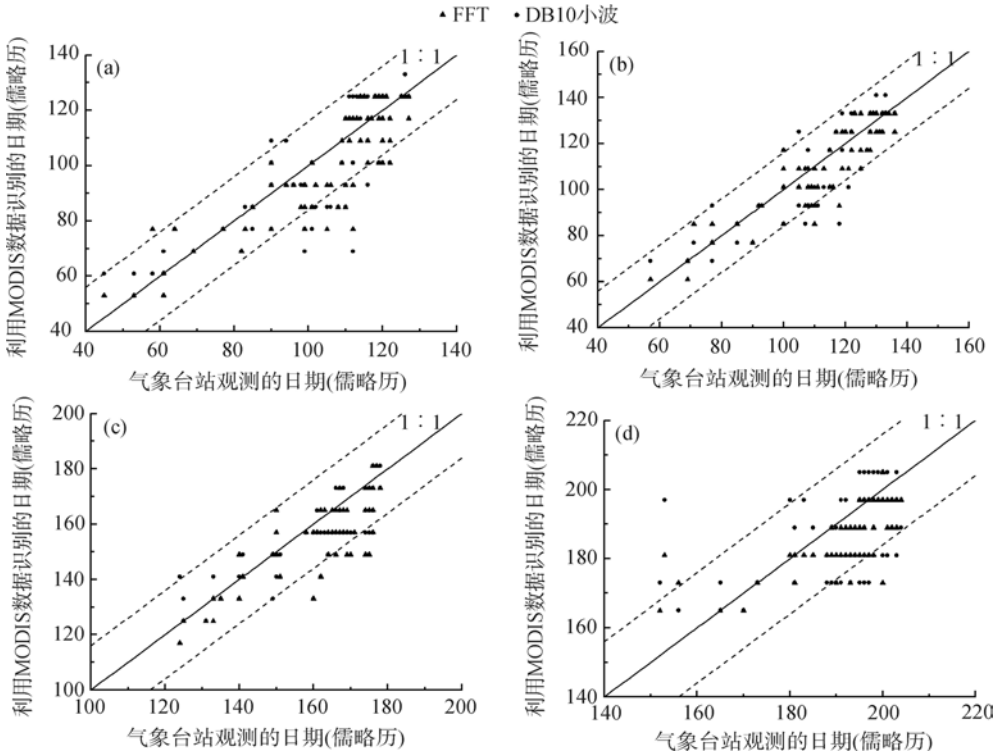

图 5 利用 MODIS 数据识别的 2005 年早稻各个生长发育期与气象台站观测的各个生长发育期的比较结果

(a)移栽期; (b)分蘖初期; (c)抽穗期; (d)成熟期(图中的虚线是误差为±16d 的边界线)

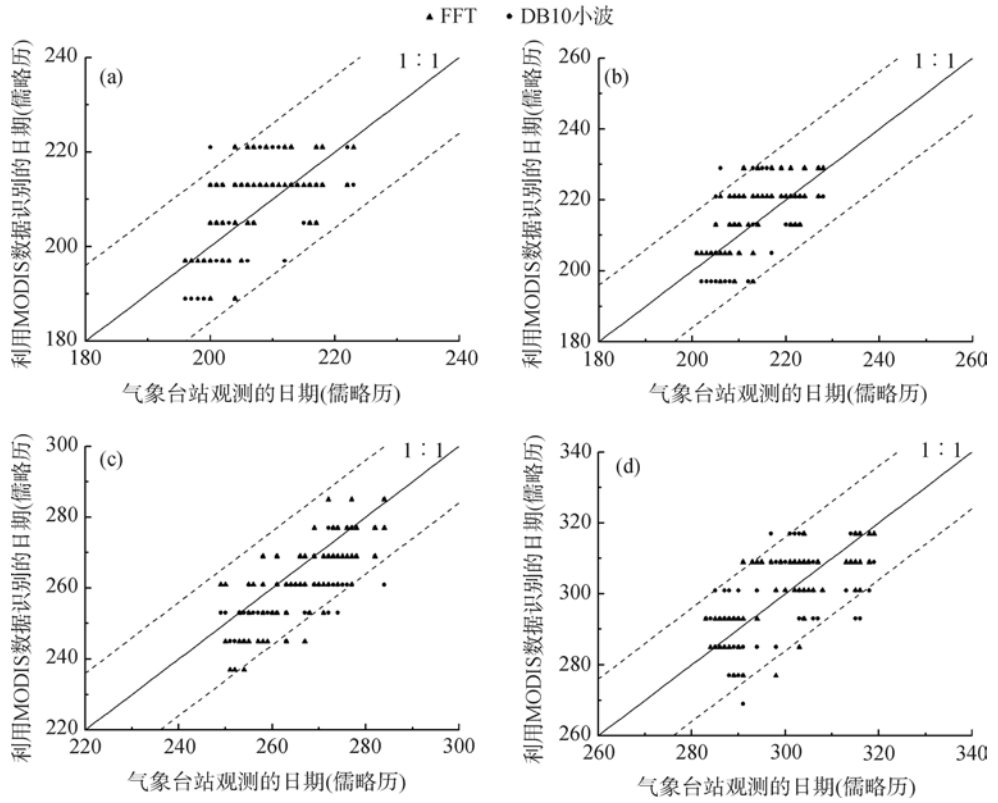

图 6 利用 MODIS 数据识别的 2005 年晚稻各个生长发育期与气象台站观测的各个生长发育期的比较结果

(a)移栽期; (b)分蘖初期; (c)抽穗期; (d)成熟期(图中的虚线是误差为±16d 的边界线)

以上分析表明, 利用 FFT 和小波变换低通滤波法去噪处理后的 EVI 识别的水稻生长发育期结果基本一致, 尽管 Sakamoto 等(2005)在获取日本的水稻季相信息研究中表明小波处理略优于傅里叶变换去噪处理的结果。研究发现在有些地区的时间序列中 EVI 受到云覆盖的影响比较严重。由于小波变换能

表 2 假设气象台站的观测数据为真值，利用 **FFT** 和小波变换低通滤波处理的时间序列 **EVI** 对水稻生长发育期识别的均方根误差比较结果

种植方式	发育期名称	FFT/d	DB10 小波/d
单季稻	移栽期	10.7	16.2
	分蘖期	11.1	15.9
	抽穗期	11.2	11.5
	成熟期	14.6	12.4
早稻	移栽期	11.6	12.6
	分蘖期	8.9	10.5
	抽穗期	9.5	10.1
	成熟期	9.6	12.9
晚稻	移栽期	7.2	9.3
	分蘖期	7.8	9.5
	抽穗期	9.3	8.8
	成熟期	7.9	10.4

够表示处理非周期和不平稳的信号，所以小波方法很可能对信号的局部变化更敏感而导致误差。由于水稻的生长发育的变化具有特别强的周期性，而 FFT 低通滤波方法对周期性强的信号的模拟是适用的，得出的结果有可能会更好些。总之，两种方法得出的结果基本接近。

4 结论与讨论

研究在对时间序列 EVI 进行傅里叶和小波低通滤波平滑后，利用不同的方法判断水稻的移栽期、分蘖初期、抽穗期和成熟期。通过分析表明以上的算法对水稻的生长发育期信息提取是有效的，然而结果中也存在着不可避免的误差。误差的来源主要包括以下 3 个方面：第一，为了降低云覆盖的影响，研究采用 8d 合成的数据代替每天获取的数据，并用这 8d 中的中间值(约第 4d)代表图像实际获取的日期，所以这样会导致获取的结果产生±4d 以内的误差。第二，气象台站的位置与本研究中抽取的样点在空间位置上并不一致，采用空间插值法获取的日期与实际值仍然存在差异，这也是产生误差的重要来源之一。第三，由于研究是采用抽样的方法获取水稻的生长发育期数据，即使在同一个相对较小的地区，由于选取的地块不同，获取的结果仍然会有差异。

通过云检测表明，即使在 8d 合成的数据中仍然存在大量被云覆盖的像元。如果采用 16d(Terra 的一个周期)合成的数据，云覆盖的影响会被进一步降低，但这样会使数据的时间分辨率变低，真实日期与代表日期的误差也会增大到±8d 以内。由于农作物的生长季一般较短，通常仅存在几个月，所以利用 16d 合成的数据识别的结果精度过低。在云覆盖较少的地区，如果采用每天获取的数据，会大大地提高其时间分辨率，识别效果可能会更好。

通过以上的比较分析表明，利用 8d 合成的 MODIS 数据识别水稻的生长发育期是可以实现的。由于时间序列的 EVI 受到云及其他因素的干扰，尽管利用 FFT 和小波低通滤波可消除绝大部分噪声，但平滑后的结果仍然受到一定的影响。通过与气象台站的地面调查资料比较，识别结果的误差绝大部分在±16d 以内，所以从整体而言结果还是可靠的。因此，可以利用研究中的方法获取其他年份的水稻生长发育期信息，为监测水稻的种植面积和长势提供参考。此外，根据其他作物的生长发育期特点，本研究中采用的算法也可能被用于提取其他作物的生长发育期。

致 谢 研究采用地面观测的水稻生长发育期资料由国家气象局气象资料室提供；MODIS 数据由美国 MODIS 陆地工作组(MODIS Land Team)提供，并从 LPDAAC (Land Processes Distributed Active Archive Center)(http://LPDAAC.usgs.gov)免费获取的。在此，对以上提供资料支持的单位表示衷心的感谢。

REFERENCES

Chen J, Jonsson P, Tamura M, Gu Z, Matsushita B and Eklundh L. 2004. A simple method for reconstructing a high-quality NDVI time-series data set based on the Savitzky-Golay filter. *Remote Sensing of Environment*, **91**: 332—344

Chen X, Tan Z J, Schwartz M D and Xu C. 2000. Determining the growing season of land vegetation on the basis of plant phenology and satellite data in Northern China. *International Journal of Biometeorology*, **44**: 97—101

Chen X, Xu C and Tan Z. 2001. An analysis of relationships among plant community phenology and seasonal metrics of Normalized Difference Vegetation Index in the northern part of the monsoon region of China. *International Journal of Biometeorology*, **45**(4): 170—177

Cihlar J. 1996. Identification of contaminated pixels in AVHRR composite images for studies of land biosphere. *Remote Sensing of Environment*, **56**: 149—153

Cooley J, Lewis P and Welch P. 1969. The finite Fourier transform . *IEEE Trans. Audio Electroacoustics*, **17**(2): 77—85

Defila C and Clot B. 2001. Phytophenological trends in Switzerland. *International Journal of Biometeorology*, **45**: 203—207

Duchemin B, Goubicr J and Courrier G. 1999. Monitoring phenological key stages and cycle duration of temperate deciduous forest ecosystems with NOAA/AVHRR data. *Remote Sensing of Environment*, **67**: 68—82

Fischer A. 1994. A model for the seasonal variations of vegetation indices in coarse resolution data and its inversion to extract crop parameters. *Remote Sensing of Environment*, **48**(2): 220—230

Gallo K P and Flesch T K. 1989. Large-area crop monitoring with the NOAA AVHRR: Estimating the silking stage of corn development. *Remote Sensing of Environment*, **27**: 73—80

Gillian L G, John F M, Jerry M , Aline G, Carlos C C and Carlos E P C. 2008. Wavelet analysis of MODIS time series to detect expansion and intensification of row-crop agriculture in Brazil. *Remote Sensing of Environment*, **112**: 576—587

Huete A R, Didan K, Miura T, Rodriguez E P R, Gao X and Ferreira L G. 2002. Overview of the radiometric and biophysical performance of the MODIS vegetation indices. *Remote Sensing of Environment*, **83**: 195—213

Huete A R, Liu H Q, Batchily K and van Leeuwen W. 1997. A comparison of vegetation indices global set of TM images for EOS-MODIS. *Remote Sensing of Environment*, **59**: 440—451

Jönsson P and Eklundh L. 2004. TIMESAT — a program for analyzing time-series of satellite sensor data. *Computers & Geosciences*, **30**: 833—845

Justice C O, Townshend J R G, Holben B N and Tucker C J. 1985. Analysis of the phenology of global vegetation using meteorological satellite data. *International Journal of Remote Sensing*, **6**(8): 1271—1318

Lloyd D. 1990. A phenological classification of terrestrial vegetation cover using shortwave vegetation index imagery. *International Journal of Remote Sensing*, **11**: 2269—2279

Lu X, Liu R, Liu J and Liang S. 2007. Removal of noise by Wavelet method to generate the high-quality time series of terrestrial MODIS products. *Photogrammetric Engineering and Remote Sensing*, **73**(10): 1129—1139

Markon C J, Fleming M D and Binnian E F. 1995. Characteristics of vegetation phenology over the Alaskan landscape using AVHRR time-series data. *Polar Record*, **31**: 179—190

Menzel A. 2000. Trends in phenological phases in Europe between 1951 and 1996. *International Journal of Biometeorology*, **44**: 76—81

Moulin S, Kergoat L, Viovy N and Dedieu G. 1997. Global-scale assessment of vegetation phenology using NOAA/AVHRR satellite measurements. *Journal of Climate*, **10**: 1154—1170

Myneni R B and Tucker C J. 1997. Increased plant growth in the northern high latitudes from 1981 to 1991. *Nature*, **386**: 698—702

NBSC (National Bureau of Statistics of China). 2007. Statistical Yearbook of China. China Statistics Press

Parmesan C and Yohe G. 2003. A globally coherent fingerprint of climate change impacts across natural systems. *Nature*, **421**: 37—42

Reed B C and Brown J F. 1994. Measuring phenological variability from satellite imagery. *Journal of Vegetation Science*, **5**: 703—714

Repo T, Hänninen H and Kellomäki S. 1996. The effects of long-term elevation of air temperature and CO_2 on the frost hardiness of Scots pine. *Plant Cell and Environment*, **19**: 209—216

Roetzer T, Wittenzeller M, Haeckel H and Nekovar J. 2000. Phenology in central Europe-differences and trends of spring phenophases in urban and rural areas. *International Journal of Biometeorology*, **44**: 60—66

Root T L, Price J T, Hall K R, Schneider S H, Rosenzweig C and Pounds J A. 2003. Fingerprints of global warming on wild animals and plants. *Nature*, **421**: 57—60

Roy D P, Borak J S, Devadiga S, Wolfs R E, Zheng M and Descloitres J. 2002. The MODIS Land product quality assessment approach. *Remote Sensing of Environment*, **83**: 62—76

Sakamoto T, Yokozawa M, Toritani H, Shibayama M, Ishitsuka N and Ohno H. 2005. A crop phenology detection method using time-series MODIS data. *Remote Sensing of Environment*, **96**: 366—374

Savitzky A and Golay M J E. 1964. Smoothing and Differentiation of data by simplified least squares procedures. *Analytical Chemistry*, **36**(8): 1627—1639

Schwartz M D, Reed B C and White M A. 2002. Assessing satellite-derived start-of-season measures in the conterminous USA. *International Journal of Climatology*, **22**(14): 1793—1805

Schwartz M D. 1999. Advancing to full bloom: planning phenological research for the 21st century. *International Journal of Biometeorology*, **42**(3): 113—118

Sellers P J, Tucker C J, Collatz G J, Los S O, Justice C O, Dazlich D A and Randall D A. 1994. A global 1° by 1° NDVI data set for climate studies: Part II. The generation of global fields of terrestrial biophysical parameters from the NDVI. *International Journal of Remote Sensing*, **15**(17): 3519—3545

Studer S, Appenzeller C and Defila C. 2005. Inter-annual variability and decadal trends in Alpine spring phenology: a multivariate analysis approach. *Climate Change*, **73**: 395—414

Tucker C J, Elgin J H Jr, McMurtrey J E and Fan C J. 1979. Monitoring corn and soybean crop development by remote sensing techniques. *Remote Sensing of Environment*, **8**(3): 237—248

Viovy N, Arino O and Belward A. 1992. The Best Index Slope Extraction (BISE): A method for reducing noise in NDVI time-series. *International Journal of Remote Sensing*, **13**(8): 1585—1590

Yu F, Price K P, Ellis J and Shi P. 2003. Response of seasonal vegetation development to climatic variations in eastern central Asia. *Remote Sensing of Environment*, **87**(1): 42—54

Zhang X, Friedl M A, Schaaf C B, Strahler A H, Hodges J C F, Gao F, Reed B C and Huete A. 2003. Monitoring vegetation phenology using MODIS. *Remote Sensing of Environment*, **84**: 471—475

Zhou L, Tucker C J, Kaufmann R K, Slayback D, Shabanov N V and Myneni R B. 2001. Variations in northern vegetation activity inferred from satellite data of vegetation index during 1981 to 1999. *Journal of Geophysical Research*, **106**: 20069—20083

附中文参考文献

中华人民共和国国家统计局(NBSC). 2007. 中国统计年鉴. 中国统计出版社